Leader Distributed Coupling of Swarmalator Systems

Avaniko Asokkumar¹ and Steven Ceron²

¹ University of Pennsylvania, Philadelphia PA 19104, USA, aavaniko@seas.upenn.edu

Abstract. This paper delves into the innovative integration of swarming and synchronization behaviors in robotics, with a focus on the swarmalator model. Through numerical studies conducted using MATLAB, the research explores the impact of distributed coupling networks on emergent behaviors. By investigating different symmetry types and the influence of leader-follower interactions, the study sheds light on the rich dynamics achievable within the swarmalator model. The analysis includes characterizing agent distributions, radius variations, and the distance traveled by the center of mass. Furthermore, the paper highlights the importance of exploring diverse coupling distributions beyond the leader network to fully tap into the model's potential. This research contributes to the ongoing exploration of the swarmalator model and its implications for future robotic systems.

Keywords: swarm robotics, swarm intelligence, emergent behavior

1 Introduction

For many years, situations have necessitated decentralized swarms of homogeneous robots [1]. While the concept of swarm robotics is not new, the combination of swarming behaviors with synchronization behaviors is still quite novel[2] [3]. O'Keefe's introduction of the swarmalator (swarming oscillator) model is the most well-grounded unification of these two phenomena [4]. While many emergent behaviors produced from the swarmalator model have been used to describe natural and biological phenomena, applications of the swarmalator model in robotics can be challenging[5] [7] [6] [8]. The most promising and practical use of the swarmalator model, however, is likely in microrobotics, where desired emergent behavior can be produced predictably with relatively few dynamic controls [9].

Within the base swarmal ator model, many studies look into the behaviors that are producible as a result of modifying certain agent-specific parameters, like the strength of attraction, synchronicity, or inherent frequency. The model is represented by equation 1. It includes tuning parameters of attraction (A) and repulsion (B) and variable parameters K and J. While A is a general global factor

² Massachusetts Institute of Technology, Cambridge, MA 02139, USA sceron@mit.edu

of attraction, and B is a global factor of repulsion (that gets strong quadratically with distance), K and J are between agents. Parameter K determines how strongly an agent attempts to synchronize its phase with surrounding neighbors. K=1 tends towards synchrony, and K=-1 tends toward asynchrony. Parameter J determines how strongly an agent moves towards another agent similar in phase. J=1 tends towards similar phase neighbors, and J=-1 tends away from similar phase neighbors.

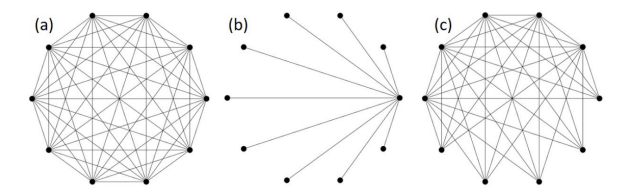
Equation 1

Equation 1
$$\dot{\boldsymbol{x}_i} = \frac{1}{N} \sum_{j \neq i}^{N} \left[\frac{\boldsymbol{x_j} - \boldsymbol{x_i}}{|\boldsymbol{x_j} - \boldsymbol{x_i}|} \left(A + Jcos(\theta_j - \theta_i) \right) - B \frac{\boldsymbol{x_j} - \boldsymbol{x_i}}{|\boldsymbol{x_j} - \boldsymbol{x_i}|^2} \right]$$

$$\dot{\theta} = \omega_i + \frac{K}{N} \sum_{j \neq i}^{N} \frac{sin(\theta_j - \theta_i)}{|\boldsymbol{x_j} - \boldsymbol{x_i}|}$$

However, there does not exist thorough literature that probes into the modification of the interaction network itself. That is modifying the coupling distribution of the network.

This paper is part of a set of studies examining distributed coupling and will examine one such network. A comparison of different distributed coupling frameworks can be seen in Figure 1, where the first is the globally coupled network, the second is the leader network, and the third is an in-between network that is similar to a multi-leader network where leaders are coupled with each other. As opposed to the globally coupled network, where all agents are coupled to all other agents, the "leader" network explored in this study couples "follower" agents to one, two, or three "leader" agents, which themselves are not directly coupled to each other.



1.1 Symmetry

This network is achieved by manipulating how the K and J parameters are applied to the agents in the swarmalator model. In the global coupling network, both K and J are set to non-zero values for all agents, but now each pairwise combination of agents may have different values and thus must be represented as K_{ij} and J_{ij} . This also allows for a form of asymmetry to be introduced beyond the high-level coupling distribution. The base symmetry assumes that $K_{ij} = K_{ji}$ and $J_{ij} = J_{ji}$, meaning the coupling strength between agents i and j is the same in both directions. Since direct follower-follower or leader-leader interactions don't happen in this network, apart from local repulsion, the coupling K and J parameters for them will be zero, while K and J for leader-followers pairs will be varied. Within just leader-follower coupling, an asymmetry can be investigated by setting $K_{Ij} \neq K_{ji} = 0$ and $J_{ij} \neq J_{jI} = 0$, or vice versa. This allows for three

different symmetry types within the leader distributed coupling network:

Symmetry 1: followers affect leaders and leaders affect followers

Symmetry 2: leaders affect followers, but followers do not affect leaders

Symmetry 3: followers affect leaders, but leaders do not affect followers.

$\mathbf{2}$ Methodology

Numerical studies were run on Matlab using Euler integration, 100 agents, a time step size of dt = 0.0025, and a final time step of tf = 40000. Each larger configuration is classified according to the symmetry type and number of leaders.

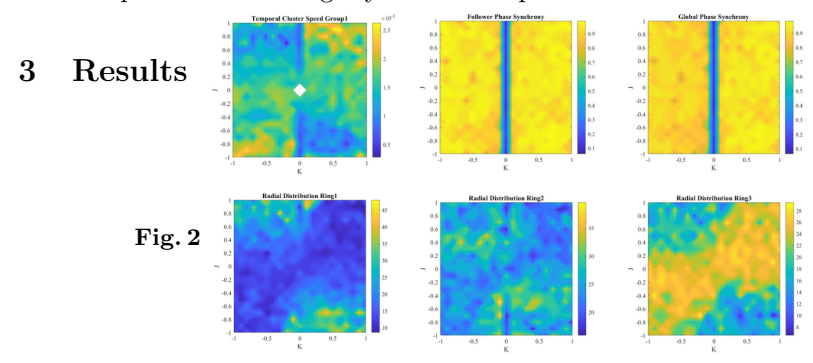
The first set of simulations use Symmetry 1, Symmetry 2, or Symmetry 3, and contain 1, 2, or 3 independent leader agents. A second set of simulations where the leader agent was given a pre-determined, and equally spaced initial phase distribution explored the effects of initial conditions on the collective dynamics. These use Symmetry 1, Symmetry 2, and Symmetry 3, and contain either 2 or 3 independent leader agents. Within the parameters set by the larger configuration, 10 trials were run per K-J configuration spaced from K = -1 to K = 1 and J =-1 to J = 1, at .1 unit intervals. This yielded 21x21 different K-J configurations.

Equation 2

Equation 2
$$\dot{\boldsymbol{x}_{i}} = \frac{1}{N} \sum_{j \neq i}^{N} \left[\frac{\boldsymbol{x}_{j} - \boldsymbol{x}_{i}}{|\boldsymbol{x}_{j} - \boldsymbol{x}_{i}|} \left(1 + J_{ij} cos(\theta_{j} - \theta_{i}) \right) - \frac{\boldsymbol{x}_{j} - \boldsymbol{x}_{i}}{|\boldsymbol{x}_{j} - \boldsymbol{x}_{i}|^{2}} \right]$$

$$\dot{\boldsymbol{\theta}} = \frac{K_{ij}}{N} \sum_{j \neq i}^{N} \frac{sin(\theta_{j} - \theta_{i})}{|\boldsymbol{x}_{j} - \boldsymbol{x}_{i}|}$$

For simplicity this study assigned all agents with a natural frequency of $\forall i, \omega = 0$, that is no inherent oscillation, and had tuning parameters of A = B =1. See Equation 2 for a slightly modified representation.



3.1 Characterization

A wide breadth of features characterizes the emergent behavior: namely physical properties, phase synchrony, collective motion, and cluster properties. For nonaccumulated data, an average of values is taken from the end of the simulation when most configurations reach a steady state. The physical properties were namely kinetic energy and both x and y direction linear momentum. The mass of each agent is modeled as one unit.

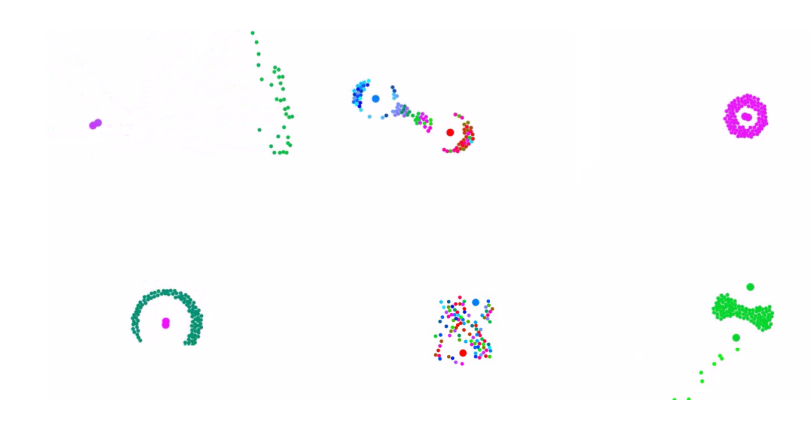
4 A. Asokkumar and S. Ceron

The synchronicity of follower agents amongst follower agents, leader agents amongst leader agents, agents within a local radius of each other, and agents across the entire system are also characterized. Phases of agents are in radians and range from 0 to 2.

We characterized the radius and distribution of agents along imagined concentric rings surrounding the center of mass (COM) and distance travelled by COM.

Arguably the behavior most unique to this coupling network is the phenomenon of clustering. We used both k-means clustering and temporal clustering to assign agents to clusters in configurations with more than 1 leader. The clusters were characterized on speed, distance traveled, and spacing of such clusters. For 2 leader configurations, a value of k=2 was used, but for 3 leader configurations, both k=2 and k=3 clustering was used. The temporal clustering classified agents based on their phase synchrony with the closest leader.

3.2 Emergent Behaviors



The behaviors found can be broadly categorized as steady or unsteady state. Steady-state behaviors move from the initial position to a final stable configuration and remain relatively unchanged over time. Unsteady state behaviors, on the other hand, involve continuous movement and changes in configuration. The first steady-state behavior is the synchronized ring (Figure 3a). This is present in both Symmetry 1 and 2 whenever there was non-zero J and K synchronization. The thickness of the ring depended on whether there was attraction between leader and follower agents. Asynchrony and negative attraction or synchrony and positive attraction led to this. The second steady-state behavior is the centric mass (Figure 3b). This occurred in the same situations that produced the synchronized ring, except that there had to be multiple leaders, and the follower agents had to be centered. The third steady-state behavior is the leader ring (Figure 3c). This behavior comes in two variations, one where the phase alignment of the leaders is equally spaced and the follower agents form a perimeter in the shape of a triangle. The second is when there are only two leaders or two of the leaders have a similar phase, and the follower agents form a curved line-like ring. Both variations are a result of no synchronization (K=0) but nonzero spatial attraction $(J \neq 0)$. The unsteady states did not have as distinctly characterizable behaviors but could be separated into two types: Convection/circulation behaviors (Figure 3d) and expansion behaviors(Figure 3e). The convection case is essentially a subset of the expansion behavior that occurs when there are at least three leaders, and followers that are expanding away from one leader go to another leader and are immediately repulsed back. This occurred more frequently in the equally spaced trials.

4 Conclusion

The findings of this study have several implications in the field of swarm robotics. While this model decides on a leader agent, the behaviors are still decentralized and self-organized, allowing for flexibility and adaptability in swarm robotics systems. One potential application may be where there is only limited external control of a swarm (i.e. one or a few leader agents) to guide the collective behavior of the entire swarm. Another potential application may lie in adversarial swarm robotics, where having a small number of leader agents can provide a strategic advantage in coordinating swarm movements and actions.

Several parameters that were investigated in previous Swarmalator papers, including natural frequency, chirality, and local coupling, were held constant in this study. The coupling distribution drastically modifies the emergent behavior associated with these swarms, so the richness associated with the Swarmalator model must be tapped into with these other parameters. Beyond the leader distributed coupling network, a methodical look into other proposed distributions is needed.

The possibilities associated with transitioning between different distributed coupling networks based on time or spatial parameters have also yet to be seen. There are many initial states that can be set rather than the random selection of phases and locations. The swarmalator remains an incredibly rich and underexplored model that would benefit from further studies.

References

- 1. Dorigo M, Theraulaz G, Trianni V (2021) Swarm Robotics: Past, Present, and Future. Proceedings of the IEEE 109(7): 1152. DOI: 10.1109/JPROC.2021.3072740
- Y. Kuramoto, "Self-entrainment of a population of coupled non-linear oscillators," in International symposium on mathematical problems in theoretical physics. Springer, 1975, pp. 420–422.
- Strogatz SH (2000) From Kuramoto to Crawford: exploring the onset of synchronization in populations of coupled oscillators. Physica D: Nonlinear Phenomena 143(1): 1-20. https://doi.org/10.1016/S0167-2789(00)00094-4
- 4. K. P. O'Keeffe, H. Hong, and S. H. Strogatz, "Oscillators that sync and swarm," Nature communications, vol. 8, no. 1, pp. 1–13, 2017
- Barciś A, Bettstetter C (2020) Sandsbots: Robots That Sync and Swarm. IEEE Access. DOI: 10.1109/ACCESS.2020.3041393

- Ceron S, O'Keeffe K, Petersen K (2023) Diverse behaviors in non-uniform chiral and non-chiral swarmalators. Nature Communications 14:940. DOI: 10.1038/s41467-023-36563-4
- 7. Ceron S, Xiao W, Rus D (2023) Reciprocal and Non-Reciprocal Swarmalators with Programmable Locomotion and Formations for Robot Swarms. IEEE Transactions on Robotics. DOI: 10.1109/TRO.2023.4567890
- 8. Ceron S, Kimmel MA, Nilles A, Petersen K (2021) Soft Robotic Oscillators With Strain-Based Coordination. IEEE Robotics and Automation Letters 6(4): 7557-7564. DOI: 10.1109/LRA.2021.3100599
- 9. Gardi G, Ceron S, Wang W, Petersen K, Sitti M (2022) Microrobot collectives with reconfigurable morphologies, behaviors, and functions. Nature Communications 13:2239. DOI: 10.1038/s41467-022-29882-5
- 10. Ceron S, Spino P, Rus D (2023) Towards Self-Organizing Swarms Composed of Swarmalators with Distributed Couplings. In: Workshop on Distributed Graph Algorithms for Robotics at ICRA 2023.